Identifying predation on rodent teeth through structure and composition: A case from Morocco

Y. Dauphin, H. Castillo-Michel, Bastien Farre, A. Mataame, K. Rbii, A. Rihane, E. Stoetzel, C. Denys

Identifying predation on rodent teeth through structure and composition: A case from Morocco

Y. Dauphin [a,*], H. Castillo-Michel [b], B. Farre [a,c], A. Mataame [d], K. Rbii [e], A. Rihane [f], E. Stoeztel [g], C. Denys [g]

[a] GDR 3591 TAPHENA, UFR TEB, Université P.& M. Curie, 4 place Jussieu, 75252 Paris cedex 05, France
[b] ID21, ESRF, 6 rue J. Horowitz, 38000 Grenoble, France
[c] UMR ISTO 7327, 1A rue de la Férolerie, 45071 Orléans cedex 2, France
[d] Institut Scientifique, Avenue Ibn Battota, B.P. 703, Agdal 10106 Rabat, Morocco
[e] Fondis Electronic, 4 rue Galilée, Quartier de l'Europe, 78285 Guyancourt, France
[f] Département des Sciences de la Vie et de la Terre, Centre Régional des Métiers de l'Education et la Formation (CERMEF), Casablanca, Morocco
[g] GDR 3591 TAPHENA,UMR ISYEB 7205, Muséum national d'Histoire naturelle, Département Systématique et Evolution, 55 rue Buffon, CP51, 75005 Paris, France

Predation by nocturnal birds of prey is one of the most frequent modes leading to the concentration of rodents in fossil assemblages. This mode of accumulation leaves characteristic surface alterations on bones and teeth. In order to evaluate and characterize the effects of these pre-diagenesis alterations on rodent fossil samples, we have carried out microstructural and chemical analyses on incisors collected from present day Moroccan wild animals and owl pellets. The microstructure of both dentine and enamel was well preserved, but chemical changes were evident in pellet samples and depended on the particular tissue and the nature of the predator. The comparison of compositional data obtained from electron microprobe chemical analyses and infrared spectrometry has allowed us to assign a possible predator to an incisor extracted from a pellet of an unknown origin. This method has further implications for the understanding of taphonomy and palaeoecology of archaeological and fossil sites.

1. Introduction

Fossil teeth often present in archaeological and palaeontological sites can be used for phylogenetic, stratigraphic and palaeoenvironmental purposes. Small vertebrate teeth are usually abundant at predation sites, especially Rodent teeth. Unfortunately, the bones and teeth of the prey are frequently mechanically and chemically modified. This first stage of changes precludes and clouds interpretation of subsequent diagenetic alterations. Using the surface bone and teeth damages due to digestion of modern samples, Andrews has distinguished five categories of predators (Andrews, 1990). These parameters have been extensively used in taphonomic studies. However, the classification proposed by Fernandez-Jalvo and Andrews (1992) does not consider the biodiversity of the existing nocturnal and diurnal predators (Denys, 2011), and some taphonomic features are shared by different predators (Fernandez-Jalvo et al., 1998). Moreover, due to the large diversity of geological environments and histories, experimental data show that it is difficult to separate between surperficial abrasion and digestion features (Fernandez-Jalvo et al., 2014). Thus, analyses of the morphological and structural alterations of digested teeth or bones are a major, but only a first step to identify the origin of the modifications.

To improve our understanding of the biological and geological origins of alterations in fossils, it is necessary (i) to enlarge the criteria and to use structural and chemical data, (ii) to compare the diagenetic behaviour of dentine and enamel, (iii) to evaluate the respective contribution of each analytical technique, (iv) to build a modern reference for future archaeological applications, and (v) to understand the effects of gastric juices upon dental tissues and bone microstructure and composition.

Enamel and dentine are apatite biocomposites, but their microstructures, organic/mineral ratios, major and minor element contents, crystallinity, etc. differ.

* Corresponding author. Tel.: +33 1 6915 6117.
E-mail addresses: yannicke.dauphin@upmc.fr, yandauph@yahoo.fr (Y. Dauphin).

For modern samples, most data have been obtained on human, bovine and rodent samples. On large samples, micro-milling permits recovery of powdered dentine and enamel, and numerous data are available in dentistry (Elliott et al., 1985; Boskey, 2007), and in palaeontology to infer their preservation state (Greene et al., 2004; Huang et al., 2007; Wang et al., 2007).

Microstructural and chemical analyses have been done to improve our knowledge of the effects of digestion. A comparison of the compositions of modern bones and teeth from rodents killed and eaten by different predators have shown that despite a well preserved inner microstructure, chemical modifications exist and differ according to the predators and the preys (Dauphin and Denys, 1988, 1992; Denys et al., 1996). Several methods are available to detect diagenetic alterations. Infrared and Raman spectrometries are among the most popular, because they provide data on crystallinity, organic matrices, Ca/P ratios, etc. (Paschalis et al., 1996; Boskey and Mendelsohn, 2005; Pasteris et al., 2008; Beniash et al., 2009; Hollund et al., 2013).

In rodents, which have small ever growing teeth, enamel covers only the labial part of the incisor, and micro-milling does not permit separation of the dentine and enamel. Moreover, digestion induces partial or even total removal of this layer (Fernandez-Jalvo and Andrews, 1992). Teeth of modern and fossil rodents were described by Korvenkontio (1934) who identified three enamel patterns: uniserial, multiserial and pauciserial. The inner layer of Muroidea incisors is built of uniserial enamel (Koenigswald, 1985). Using thin sections of rat incisors, Weber (1965) has described the special structure of the enamel adjacent to the dentine, the "remarkable repeat pattern" of the enamel rod in the inner layer of enamel, and the "highly fibrous appearance" of the outer layer. Then, the two-layered enamel was repeatedly described in modern and fossil rodents (Wahlert, 1968; Boyde, 1978; Martin, 1997). An enamel rod or prism is composed of small elongated crystals (Warshawsky, 1971).

Many palaeontological sites in North Africa have yielded numerous rodent remains whose accumulation origins by predation are suggested in absence of taphonomic analyses (Geraads, 1998; Jaeger, 1977; Lopez-García et al., 2013; Reed and Barr, 2010). In the Temara region (Morocco), continuous stratigraphic sequences (~120,000 to ~6000 BP; Nespoulet et al., 2008; Jacobs et al., 2012; Janati et al., 2012; Stoetzel et al., 2014) have yielded an abundant small faunal assemblage whose taphonomic studies have high-lighted the importance of predation (Stoetzel et al., 2011) but highlighted the lack of references concerning modern North African predators (Stoetzel and Denys, 2009). The identification of a predation bias in fossil micromammal assemblages is crucial to gain more precise information in the knowledge of the taphonomic history of sites formation as well as palaeoecological reconstructions (Andrews, 1990).

To better characterize the diagenetic processes in the archaeological caves located in Morocco, we need to build databases on modern fresh and digested samples before comparing them to fossil material. Some studies have already been undergone on bones (Dauphin et al., 2012; Farre et al., 2014). A first step is to increase references by comparing the enamel and dentine of two modern genera (*Rattus*, *Meriones*). A second step aims to characterize the effects of predation on both microstructure and chemical composition of *Meriones* incisors extracted from modern regurgitation pellets. In rodent incisors the dentine is not covered, not "protected" by the enamel, so that these teeth are a good choice to compare the diagenetic behaviour of the two tissues. In the present work, these comparisons evaluate the ability of infrared spectrometry (FTIR) and chemical analyses to detect the early diagenesis induced by the digestion. A single criterion is not sufficient to infer the state of preservation. Thus, the microstructure, UV fluorescence, quantitative and qualitative chemical analyses, and FTIR observations have been performed.

2. Material and methods

2.1. Material

Incisors were extracted from modern *Rattus sp.* bred at the Museum national d'histoire naturelle (Paris) and *Meriones shawii*. Both genera are Muridae, but *Rattus* is a Murinae and *Meriones* is a Gerbillinae, so that shapes of molars greatly differ. Thus, we used only incisors because they have similar shapes to avoid additional biases. *Meriones* teeth from Morocco have different histories and origins. Two teeth were from wild living animals, while others have been collected in regurgitation pellets. One pellet is from *Bubo ascalaphus* from Guenfouda (near Oujda), another one was from an undetermined owl (*Tyto alba*? from Ouled Boughadi, Central part of Morocco). At last, two other pellets are from unknown predators (Table 1).

2.2. Cleaning – inclusion processes

The residual flesh and possible contaminants (bacteria) were destroyed using Na hypochlorite (dilute commercial solution) at room temperature and an ultrasonic bath. Samples were then rinsed with tap water and air dried. Incisors were mounted in epoxy resin and polished to a 0.25 μm finish using diamond paste. The exposed surface is through the long axis of the tooth, so that enamel and dentine are exposed on the same section. The same teeth were used for microstructural and compositional analyses.

2.3. Scanning electron microscopy

Polished sections and fractured samples were etched to reveal microstructural features. SEM observations were conducted using a Philips SEM XL30 in secondary electron mode (25 kV accelerating voltage), and a Phenom ProX in back scattered electron mode (BSE) (15 kV accelerating voltage). Details of sample preparations are given in the figure legends.

2.4. UV fluorescence

The epifluorescence signal of polished surfaces was observed under ultraviolet light using a Zeiss Standard microscope equipped with Neofluar fluorite objectives, a Zeiss mercury lamp, excitation filter (365 nm), and a transmission cut-off filter (400 nm).

Table 1
Origin of studied samples.

Origin (Morocco)	Predator	Species	Teeth: incisors	Surface modifications
MNHN (bred in captivity)	Fresh material	Rattus sp.	1	No modification
Ben Guerir	Fresh material	*M. shawii*	2 left lower – cut in situ	No modification
Ouled Boughadi	Owl indet.	Meriones	1 isolated right upper	Non digested
Guenfouda	*B. ascalaphus*	Meriones	1 isolated right lower	Broken, non digested
Unknown	Unknown	Meriones	2 isolated left lower	Very light digestion

2.5. Fourier transform infrared microscopy

The synchrotron infrared microscopy was performed on the FTIR end-station of the ID21 beam line at the European Synchrotron Radiation Facility (ESRF). This beam line is equipped with a Continuum IR microscope (Thermo Nicolet) coupled to a Nexus FTIR bench (Thermo Nicolet). The microscope was operated in reflection mode, where the focusing Schwarzschild objective has a magnification of 32× (NA = 0.65). Due to its reduced source size and high collimation properties, a synchrotron IR source allows signal-to-noise ratios to be kept at diffraction-limited resolutions. The microscope is equipped with a computer-controlled *x*/*y* stage allowing acquisition of profiles or maps of the sample. Maps were scanned with steps of 4 μm in both directions, with an aperture size of $5 \times 5\ \mu m^2$. Spectra were collected in reflection mode, with a resolution of $8\ cm^{-1}$. For each spectrum, 250 scans were accumulated in the wave-number range 4000–750 cm^{-1}. Longitudinal polished surfaces were cleaned using a dilute acetic acid solution (1% for 5 s). The final format of the data was recorded as absorbance values.

Maps integrating the area from 900 to 1200 cm^{-1} ($\nu 1$, $\nu 3$ PO_4 bands) and between 1580 and 1720 cm^{-1} (amide I bands) were obtained using PyMCa software. They were then ratioed to calculate the mineral to organic matrix ratios (Paschalis et al., 1996), using Image J or Corel Paint and providing identical results.

2.6. Chemical analyses

Samples were prepared by being embedded in resin and polished with diamond pastes. The surface was then lightly etched in 5% formic acid for 15 s in order to reveal any structural details within the samples (e.g., different structures) so that the analysis positions could be related to any observed structural features. Quantitative chemical analyses were performed on an electron microprobe by using energy-dispersive techniques, with the use of a Philips XL30 SEM equipped with a solid-state X-ray detector. Analyses were done by using the Iridium analysis system using an IXRF systems Silicon drift Detector with 10 mm^2 surface area, program which estimates peak-to-background ratios. Results are given in ppm after matrix correction of the raw intensity data ($\phi - \rho$-z). A minimum of 10 analyses was made on each tissue. Measurements were made by using a live time of 120 s. Operating conditions were an accelerating voltage of 15 kV and a spot size of 5–7 μm.

The light etching done for quantitative analyses does not reveal the microstructural details of the enamel and dentine layers. Thus, an additional etching was done (5% formic acid for 15 s) so that the orientation of prisms and their inner fibrous arrangement become visible. Qualitative distribution maps were done using a Phenom PRO X equipped with the EID software; operating conditions used were 15 kV accelerating voltage, a dwell time of 150 ms and a 256 pixels resolution.

Elements analysed were Na, Mg, S, Cl, Fe, Mn, K, P, Ca, and Sr.

2.7. Statistical analyses

An attempt to separate fresh and pellets samples was done using multivariate analyses (star symbol plot) with the software Statgraphics based on (i) the ratios calculated from FTIR maps, and (ii) the elemental chemical analyses.

The chemical compositions of 10 localized analyses were averaged for each tissue of every tooth. The results are given in Table 2. Thus, 30 analyses have been done for the enamel and dentine of three fresh *Meriones*, and 40 analyses for four *Meriones* extracted from pellets. To estimate the variability of the chemical composition of the tissues, the standard deviation (sd: Table 2) has been calculated. Standard deviation can be calculated from punctual analyses (10, 30 and 40), or from number of individual (1, 3 and 4). We used the number of individuals, so that standard deviations are higher than those calculated from punctual analyses.

3. Results

3.1. Microstructure

The spatial arrrangement of prismatic units in mammal enamel has been described by several authors, using various criteria (Fig. 1, Fig. S1). All studied samples exhibit the typical uniserial structure of the Muroidea enamel. Uniserial is a term "only used in rodent incisors and molars" and "consist of layers one prism thick" (von Koenigswald and Sanders, 1997) (Fig. S1).

3.1.1. Fresh samples

The lower incisor of *Rattus* comprises two layers: dentine and enamel (Fig. 1a). Two sublayers of enamel are visible, the outer sublayer (EOL) being thin (Fig. 1a, b). The enamel inner layer (EIL) is very thick and uniserial (Fig. 1a, c). The dentinal tubules are regular, more or less empty depending on the preparation and freshness of the tooth (Fig. 1d). The structure of the lower incisor of *Meriones* is similar (Fig. 1g–i): the enamel outer layer is thin (Fig. 2e), while the uniserial pattern of the inner layer is well visible (Fig. 1f, g). The prismatic units are composed of parallel elongated fibres. Depending on the orientation of the section, dentine tubules are more or less oval (Fig. 1h, i).

3.1.2. Samples extracted from regurgitation pellets:

The outer surface of incisors ingested by *B. ascalaphus* is not strongly altered (Fig. 2a–c). Altered zones show the layered structure of the enamel (Fig. 2b) and the enamel dentine junction

Table 2
Chemical composition (ppm) of enamel and dentine of Rodent teeth. FE: fresh enamel, FD: fresh dentine, PE: enamel from a tooth extracted from a regurgitation pellet; PD: dentine from a tooth extracted from a regurgitation pellet; ni: number of teeth; na: number of punctual analyses; m: mean; sd: standard deviation.

			Na	Mg	S	K	Cl	Fe	Sr	Mn	Ca	P	Ca/P	Taxa
FE	ni = 3	m	7982	2467	21	589	3479	1127	4133	812	299,401	170,502	1.75	Meriones
	na = 30	sd	720	715	5	182	161	167	288	176	16,413	7513		
	ni = 1	m	7927	4252	449	895	3450	2156	3471	1794	226,368	148,767	1.52	Rattus
FD	ni = 3	m	5241	16,803	1103	1229	733	966	4272	911	252,577	157,006	1.61	Meriones
	na = 30	sd	962	4696	482	271	501	214	513	277	38,412	17,024		
	ni = 1	m	4217	10,386	409	594	1989	968	1711	763	137,134	95,603	1.43	Rattus
PE	ni = 4	m	8368	1753	57	489	3933	909	4234	691	287,184	163,937	1.75	Meriones
	na = 40	sd	693	102	82	177	241	166	429	151	39,950	16,319		
PD	ni = 4	m	4455	15,222	1684	1080	841	775	3068	544	166,664	115,026	1.45	Meriones
	na = 40	sd	981	4821	485	328	541	134	1096	78	68,481	36,210		

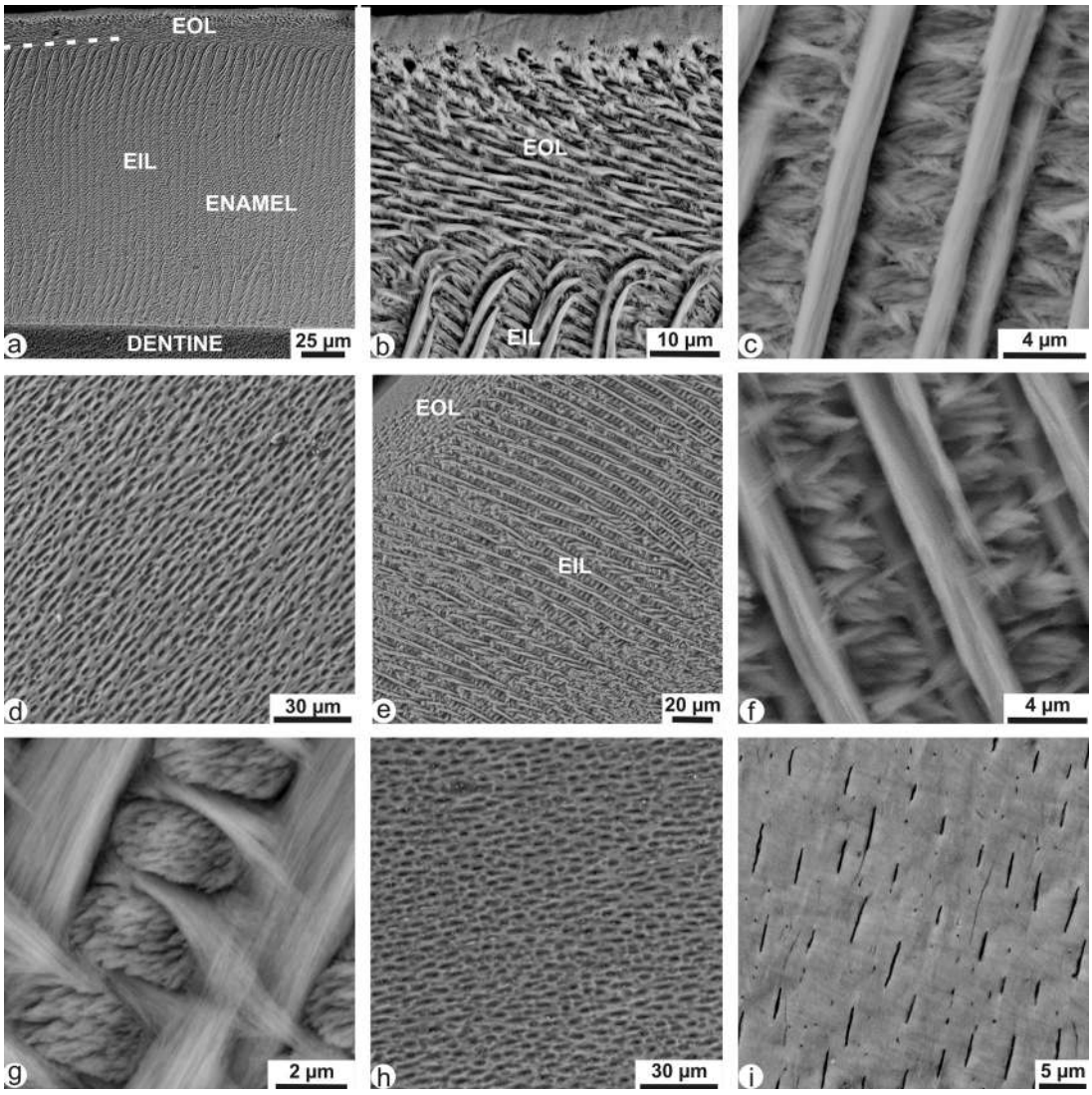

Fig. 1. Structure of fresh incisors – scanning electron microscope (SEM), back scattered electron (BSE) images.
a–d: *Rattus*, polished and etched section (formic acid 5% for 10 s); a – Parasagittal polished section showing the enamel outer (EOL) and inner (IEL) layers. b – Detail of the structure of the outer layer of enamel. c – Uniserial pattern of the EIL. d – Oblique section shows the tubules in dentine.
e–i: *M. shawii*; e – Parasagittal section showing the two sublayers in the enamel (HCL 1% for 30 s). f – Detail of the same showing the uniserial pattern of EIL. g – Parasagittal section of another incisor showing the uniserial pattern of the EIL and the parallel fibres within a prism (HCl 1% for 15 s). h – Same sample, tubules in the dentine. i – Oblique section of the dentine, showing the tubules (formic acid 5% for 10 s).

(Fig. 2c). Dentinal tubules are empty (Fig. 2d). Longitudinal sections, polished and etched, do not show alteration (Fig. 2e–i). The outer layer of the enamel is present and its structure preserved (Fig. 2e, f), and the uniserial pattern of the inner layer shows the series of prims composed of parallel fibres (Fig. 2g). The structure of the dentine is not modified (Fig. 2h, i).

The outer surface of teeth from the unidentified owl regurgitation pellet is less digested than those of *B. ascalaphus*. Only some thin furrows on enamel (Fig. 3a, b), and polygonal cracks on dentine (Fig. 3c) are visible. Longitudinal sections show a well-preserved structure of the enamel and dentine (Fig. 3d–f).

Incisors from unidentified pellets also show well-preserved structures of the enamel and dentine (Fig. 3a–f). In one tooth, dentinal tubules are not empty (Fig. 3f).

From a microstructural point of view, the inner structures of both fresh and pellet teeth are similar. There is no distinctive sign of digestion.

3.2. Bulk composition

UV fluorescence images on polished unstained sections show the difference between enamel and dentine in all the samples, fresh (Fig. S1a–d) or extracted from pellets (Fig. S1e–i). The uniserial structure of the inner layer of the enamel is visible, as well as the two enamel layers (Fig. S1b, f, h), but apart the microstructure, there is no difference between EOL and IOL. From these data, it is not possible to distinguish between fresh and pellet samples.

Infrared maps have been done on sections including enamel and dentine. On thick teeth, only a part of the enamel layers was analysed. Some bands are displayed: 878 cm^{-1} ($\nu 2$) and 1457 cm^{-1} ($\nu 3$) for CO_3, 961 cm^{-1} ($\nu 4$), 1020 and 1100 cm^{-1} ($\nu 3$) for PO_4, 1238 cm^{-1} for amide III, 1543 cm^{-1} for amide II and 1652 cm^{-1} for amide I.

In *Rattus* incisor, $\nu 2$ CO_3 (878 cm^{-1}), $\nu 4$ (961 cm^{-1}) and $\nu 3$ (1020 cm^{-1}) PO_4 maps are similar (Fig. 4b–d): dentine and enamel

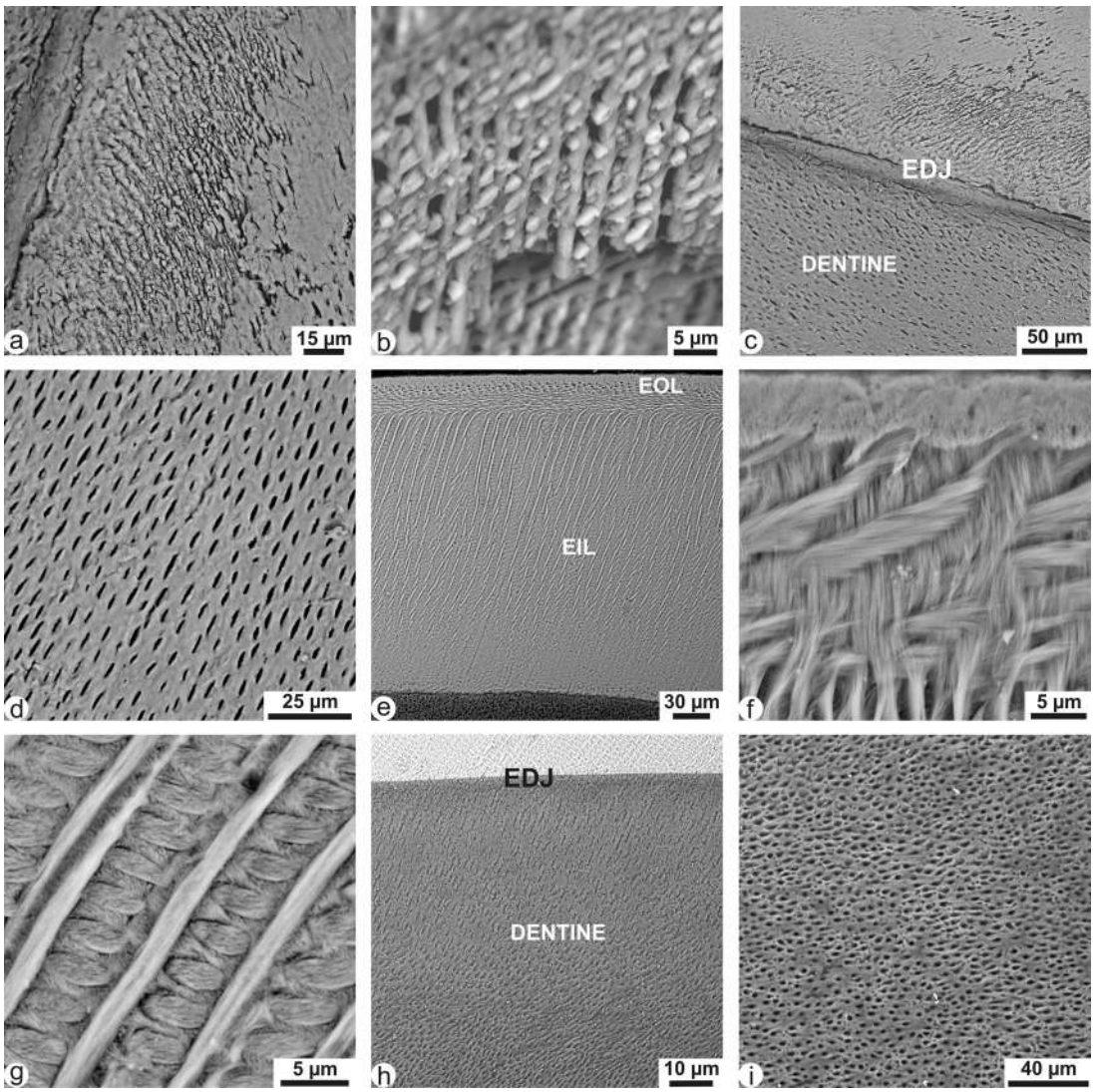

Fig. 2. Structure of *Meriones* incisors extracted from regurgitation pellets of *Bubo* – SEM BSE images.
a–d: Untreated samples. a – Outer surface showing the structure of the altered enamel. b – Fracture showing the uniserial pattern of the enamel. c – Altered outer surface showing the enamel dentine junction (EDJ). d – Fracture showing the tubules of the dentine.
e–i: Polished and etched section (HCl 1% for 30 s); e – Parasagittal section showing the two sublayers (EOL and EIL) of the enamel. f – Detail of the outer layer of enamel. g – Detail of the uniserial pattern of EIL. h – EDJ and dentine, showing the parallel tubules. i – Detail of the tubules of the dentine.

differ, and the EDJ (Enamel Dentine Junction) zone is clearly visible. The lateral change in colour (from yellow on the left to the green on the right for the dentine) is probably due to a decrease in the synchrotron beam during the acquisition. The difference between the tissues is stronger for the 1100 cm^{-1} band (ν3 for PO_4, Fig. 4e), whereas it is weaker for the ν3 CO_3 band (1457 cm^{-1}, Fig. 4g). The main organic band (amide I, 1652 cm^{-1}, Fig. 4i) does not show difference between enamel and dentine, despite the EDJ is distinct. Amide III band (1238 cm^{-1}) displays more differences in the organic content of enamel and dentine. Nevertheless, a precise assignment of these organic bands is not possible.

Similar observations were done on a fresh *Meriones* incisor (Fig. 4j, k). It can be seen that the main orientation of the uniserial pattern is displayed from some wavelengths (Fig. 4k, q). In all maps, the EDJ is thin and well characterized. Dentine maps show large zones from the EDJ towards the pulp cavity, in agreement with what can be seen in microstructures. Similarly the 1100 cm^{-1} band (ν3 PO_4) shows the change in the dentine near the EDS (Fig. 4m), and the amide III band shows some changes in the enamel composition near the EDJ (Fig. 4n).

The differences between enamel and dentine are weaker in the tooth extracted from a regurgitation pellet of *Bubo* as shown by the colours restricted to a blue range in most maps (Fig. 5a–h). Nevertheless, the main differences are also displayed by the 1100 cm^{-1} and 1238 cm^{-1} bands (Fig. 5d, e). Faint changes are visible in dentine, from the outer zone (near the enamel) towards the pulp cavity. EDJ is visible in all maps, but is sharp.

The range of colours in infrared maps of the incisor extracted from a pellet of an unidentified owl is very different (Fig. 5i–p). The three first maps (878, 961 and 1020 cm^{-1}) are not similar as they are in the previous samples (Fig. 5i–k). Only a faint colour difference between enamel and dentine is displayed at one of the main PO_4 band (961 cm^{-1}) (Fig. 5j). The main features of incisors of pellets of unknown predators are similar (data not shown).

From FTIR maps, spectra can be extracted and various ratios calculated. Moreover, maps of the area of the ν1–ν3 phosphate bands (900–1200 cm^{-1}), and of organic bands (amide I–II between 1580 and 1720 cm^{-1}) can be also obtained and ratioed.

The 1030/1080 cm^{-1} ratio was used to estimate the crystallinity of both dentine and enamel (Fig. S2a). *Rattus* exhibits a strongest

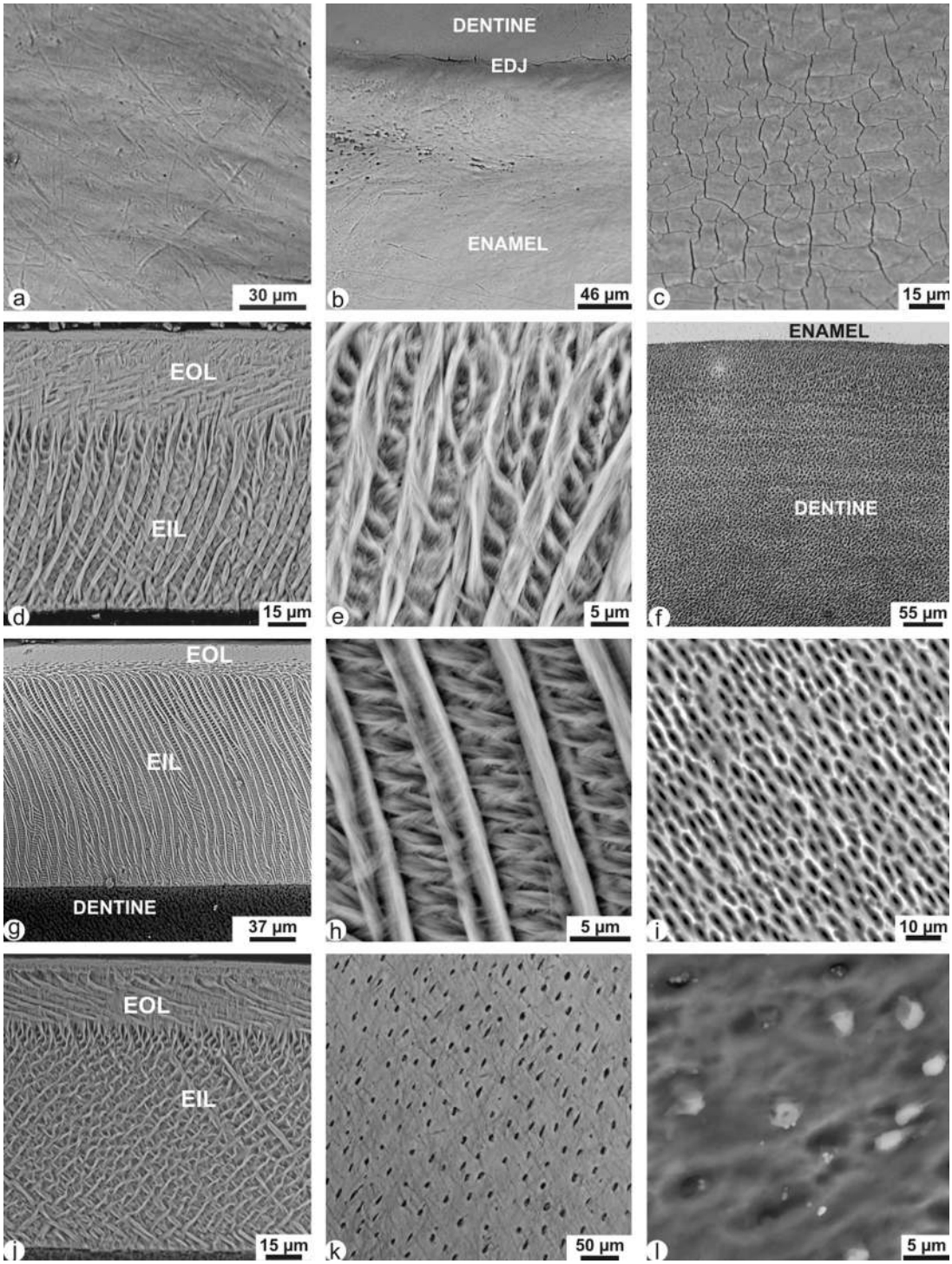

Fig. 3. Structure of *Meriones* incisors extracted from regurgitation pellets – SEM BSE images.
a–f: Incisor from owl pellet; a–c: Untreated outer surface. d–f: Parasagittal polished and etched section (HCl 0.01 M for 5 s). a – Outer surface of the enamel near the tip of the tooth; the structure of the enamel is not visible. b – Outer surface around the EDJ junction. c – Polygonal cracks on the outer surface of dentine. d – Sections showing the change in the prism orientation in EOL and IEL. e – Detail of the uniserial pattern of EIL. f – Tubules and growth lines in dentine.
g–i: Polished and etched parasagittal section of a *Meriones* incisor collected in a pellet from an unknown bird of prey (HCl 1% for 15 s). g – Dentine and sublayers (EOL, EIL) of enamel are visible. h – Detail of the uniserial pattern in EIL. i – Tubules in dentine are empty.
j–l: Polished and etched parasagittal section of another *Meriones* incisor collected in a pellet from an unknown bird of prey (formic acid 5% for 10 s). j – Uniserial pattern of the inner sublayer of enamel (EIL), and outer sublayer (EOL). k – Empty dentinal tubules. j – Some dentinal tubules are still filled with cellular processes.

crystallinity for enamel, as well the strongest difference between the two tissues. Enamel of *Meriones* is more crystalline that the dentine in fresh and pellet samples, except for one tooth. The ratio between the carbonate and phosphate bands of the *Rattus* enamel is the strongest one, and the difference between enamel and dentine is also the strongest of all the studied samples (Fig. S2b). From this point of view, in all pellet teeth, this ratio is higher in dentine than in enamel.

To estimate the organic–mineral ratios, two amide bands (A and I) and two mineral bands (carbonate and phosphate) were used (Fig.

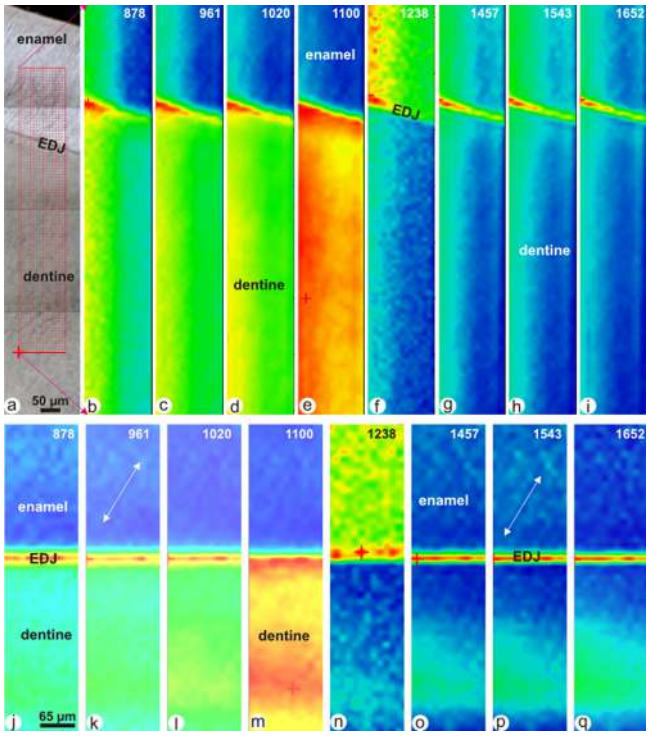

Fig. 4. FTIR maps of fresh incisors – polished parasagittal sections. EDJ: Enamel dentine junction.
a–i: *Rattus*. a – Location of the maps. b – $\nu 3\ CO_3$ band. c – $\nu 1\ PO_4$ band. d – $\nu 3\ PO_4$ band. e – $\nu 3\ PO_4$ band showing the main difference between enamel and dentine. f – Amide III band. g – $\nu 3\ CO_3$ band. h – Amide II band. i – Amide I band.
j–q – *Meriones*. j – $\nu 3\ CO_3$ band. k – $\nu 1\ PO_4$ band. l – $\nu 3\ PO_4$ band. m – $\nu 3\ PO_4$ band showing the main difference between dentine and enamel. n – Amide III band: enamel and dentine differ. o – $\nu 3\ CO_3$ band. p – Amide II band. q – Amide I band. R – Arbitrary colour scale of FTIR maps.

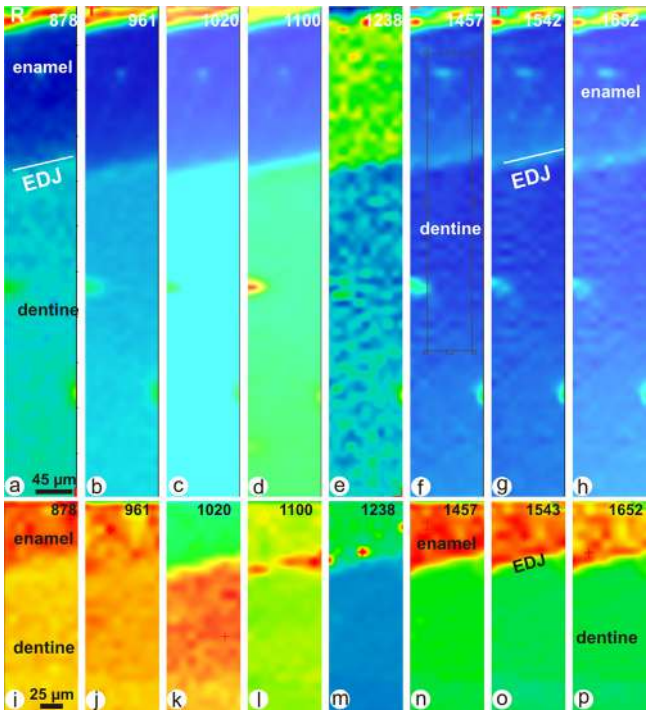

Fig. 5. FTIR maps of *Meriones* incisors extracted from pellets – polished parasagittal sections. EDJ: enamel dentine junction. R: resin.
a–h: Pellet from *Bubo*. a – $\nu 3\ CO_3$ band. b – $\nu 1\ PO_4$ band. c – $\nu 3\ PO_4$ band. d – $\nu 3\ PO_4$ band. e – Amide III band showing the main difference between enamel and dentine. f – $\nu 3\ CO_3$ band. g – Amide II band. h – Amide I band.
i–p: Pellet from an unknown owl. i – $\nu 3\ CO_3$ band. j – $\nu 1\ PO_4$ band showing a faint difference between enamel and dentine. k – $\nu 3$ PO4 band. l – $\nu 3\ PO_4$ band. m – amide III band. n – $\nu 3\ CO_3$ band. o – Amide II band. p – Amide I band.

S2c–f). Again, *Rattus* differs from *Meriones*. In ratios using the CO_3 band, the organic content is higher in dentine than in enamel in *Rattus*, in agreement with what is known for these tissues. Nevertheless, in all *Meriones* teeth, fresh and from pellets, the ratio is higher in enamel for amide A/carbonate (Fig. S2c), and higher in dentine for amide I/carbonate (Fig. S2d). For ratios based on the phosphate bands (S2e, f), *Rattus* is again clearly different from *Meriones*. Teeth extracted from pellets are similar. I/CO_3 variability is low (Fig. S2d).

The differences in the organic composition between enamel and dentine were estimated by amide I/amide A, and amide/amide II ratios (Fig. S2g, h). In all tissues and all samples, *I*/*A* ratio is higher in enamel than in dentine, except for *Rattus*, and the variability is low. Amide I/amide II ratio is more variable, and higher in dentine than in enamel, except for one pellet tooth.

From these ratios, *Rattus* is different from the fresh *Meriones*, and one of the *Meriones* extracted from a regurgitation pellet differs.

A global estimation of the mineral and organic contents of the teeth is obtained from area maps: from 900 to 1200 cm^{-1} for the mineral bands (phosphate), and from 1580 to 1720 cm^{-1} for amide bands (Boskey and Pleshko Camacho, 2007). The differences between enamel and dentine in phosphate contents are clearly displayed in fresh and pellet samples (Fig. 6a, d, g), whereas the EDJ is faint in the incisor from the *Bubo* pellet. The organic contents of dentine and enamel differ in *Rattus* (Fig. 6b), one of the fresh *Meriones* and the incisors of pellets of unknown predators. Differences are faint in other teeth (Fig. 6e, h). From the organic–mineral ratio calculated from these maps, enamel and dentine differ in all samples (Fig. 6c, f, i).

The star symbol plot based on the ratios clearly shows the heterogeneity of the enamel of fresh teeth (Fig. 7a), whereas the dentines of the two *Meriones* are similar. The low crystallinity of the dentine of *Rattus* is evidenced in this graph. Enamel and dentine from the incisors of *Bubo* pellet and of an unknown predator are similar.

3.3. Chemical composition

The elemental distribution maps of *Rattus* incisor show the difference between enamel and dentine, for both major (Ca, P) and

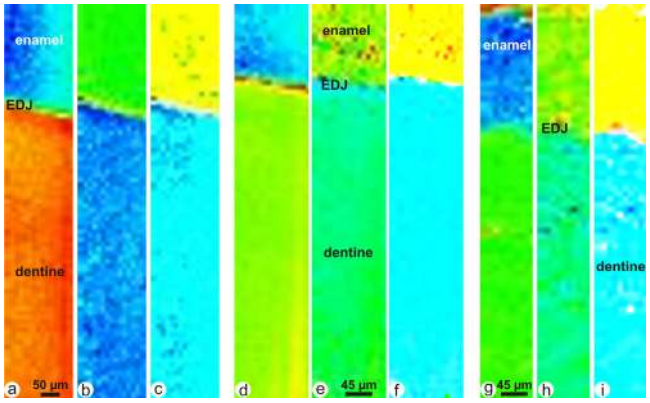

Fig. 6. FTIR maps of area between 900 and 1200 cm^{-1} for the mineral content (PO_4) (a, d, g), between 1580 and 1720 cm^{-1} for organic content (b, e, h). These maps are ratioed to estimate the mineral–organic ratios (c, f, i). a–c: *Rattus*, d–f: fresh *Meriones*, g–i: pellet from *Bubo*. The organic contents of both fresh and pellet *Meriones* differ from that of *Rattus*.

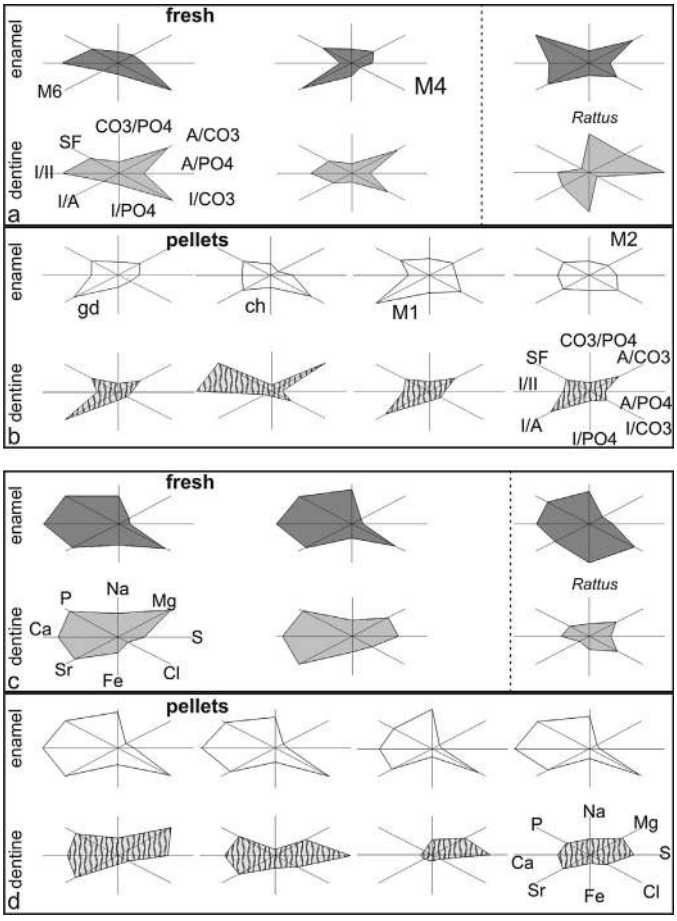

Fig. 7. Multivariate analyses (star ray plot) of dentine and enamel of incisors. a: Star ray plot based on FTIR ratios of fresh teeth of *Meriones* (M6, M4) and *Rattus*. b: Star ray plot based on FTIR ratios of teeth of *Meriones* (M6, M4) and *Rattus* extracted from regurgitation pellets. c: Star ray plot based on the chemical composition of fresh teeth of *Meriones* (M6, M4) and *Rattus*. d: Star ray plot based on the chemical composition of teeth of *Meriones* (M6, M4) and *Rattus* extracted from regurgitation pellets. The maximal value of each data is standardized to be equal to 1.

some minor elements (Fig. 8). Ca, P, Na, Sr and Cl contents are higher in enamel, whereas dentine is richer in Mg. The structure and composition of dentine layer near the enamel slightly differ from those of the main part of the dentine (Fig. 8a–d, f, g). The outer layer of the enamel is also different in structure and composition. The inner prismatic structure and the orientation of the prisms of the main part of the enamel are visible, except Cl. Similar results were obtained for the fresh *Meriones* (Fig. 9a–f) and the incisor extracted from the *Bubo* pellet (Fig. 9g–l). It must be noticed that despite the low K contents of both enamel and dentine, distribution maps

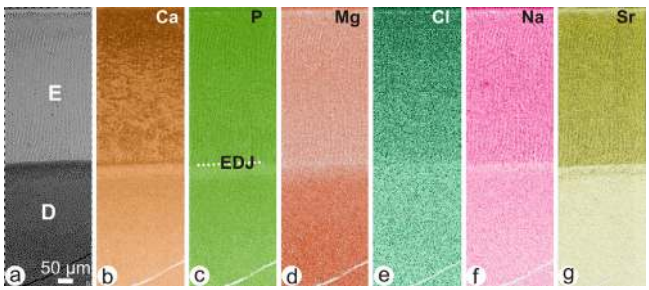

Fig. 8. Distribution maps of major (P and Ca) and some minor elements in the incisor of *Rattus*. EDJ: dentine enamel junction. Enamel is rich in Ca, P, Cl, Na and Sr contents. Dentine is rich in Mg and K.

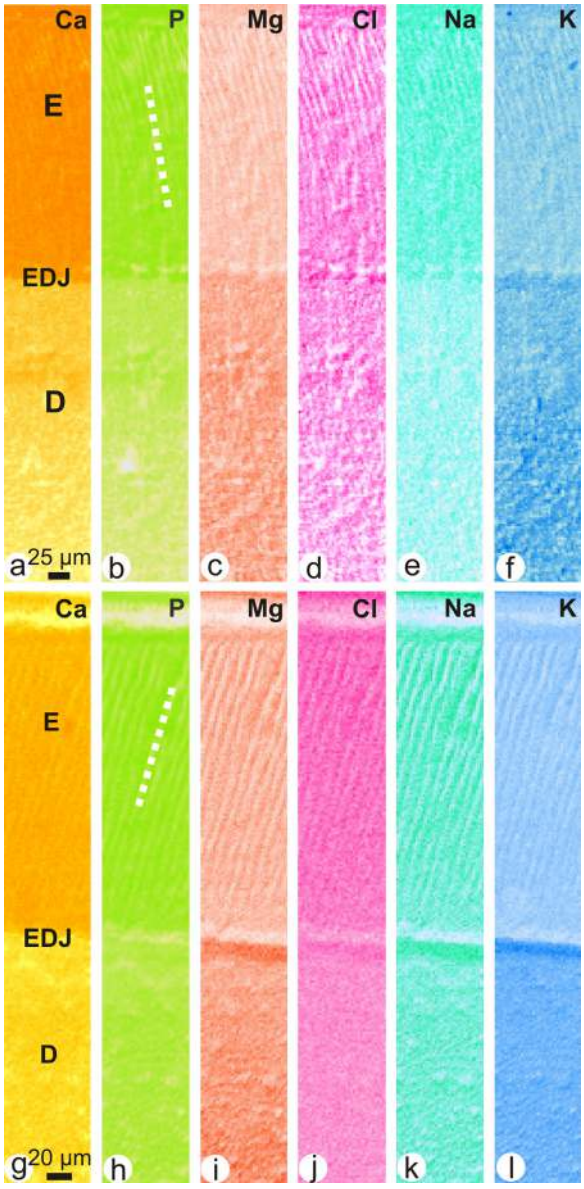

Fig. 9. Distribution maps in the incisor of a fresh *Meriones* (a–f), and one extracted from the *B. ascalaphus* pellet (g–l). In most maps, the inner structure of the enamel is still preserved.

clearly show the main features of these tissues (Fig. 9f, l). Structural changes at the EDJ correspond to chemical changes in fresh and pellet teeth.

The comparison of fresh enamel and dentine shows that *Rattus* has lower P and Ca contents than those of the wild *Meriones* (Table 2). It is a usual feature when bred animals are used. In *Meriones*, enamel is rich in Na and Cl, whereas dentine is rich in Mg and S. Like in modern animals, K, Fe and Mn are low (Fig. S3). Ca/P weight ratios are higher in enamel than in dentine, and higher in *Meriones* than that of *Rattus*. Dentine and enamel of teeth extracted from regurgitation pellets show similar features. However, all tissues are depleted in P, Ca (Table 2). Dentine is depleted in Mg, whereas enamel is enriched in Na and Cl. Ca/P ratios are similar in fresh and pellet enamels, but that of the pellet dentine is low when compared to that of the fresh dentine (Table 2).

The enamel of *Rattus* differs from that of the fresh *Meriones*, mainly because of the Fe content (Fig. 7d). Dentine is more heterogeneous. The enamels extracted from the pellets are similar (Fig. 9b), and the differences with the fresh *Meriones* are weak from

this point of view. The dentine of pellets is more diverse and more altered.

4. Discussion

4.1. Relevance of the analytical techniques

Optical and electron microscopies provide distinct data. Autofluorescence optical characteristics of enamel and dentine differ, mainly because of the organic components. However, without the use of fluorescent molecules, it is not possible to assign the difference to the composition or the quantity of the organic components: the dentine is rich in organic matrices, mainly collagen, whereas the enamel has a low organic content and is poor in collagen. SEM images provide more details about the inner structure of the tissues and the use of BSE mode confirms that the enamel is rich in mineral components.

Compositional data have been obtained using EDS and FTIR analyses. Again, these techniques are not redundant as shown by the star symbol analysis (Fig. 7). EDS allow distribution maps and quantitative analyses of elemental chemical elements, FTIR maps show the distribution of molecules through the vibration of their chemical bonds. From FTIR maps, various ratios can be known about the organic and mineral components. To work on polished surfaces is convenient because all these analyses can be done on the same samples, with a precise control of the location.

4.2. Predators and predation effects

B. ascalaphus is a nocturnal bird of prey in semi arid to arid zones. The size of the pellets varies from 25 to 74 mm, and they contain 2–5 preys. Up to 39 species are eaten by this species in Algeria (Beddiaf, 2012; Biche et al., 2001; Boukhamza et al., 1994; Sekour et al., 2010a) and Morocco (Lesne and Thévenot, 1981; Vein and Thévenot, 1978). This predator can be considered as a potential accumulator of micromammals: rodents represent about 53% of the preys and *Meriones* is dominant (Sekour et al., 2010b). Similar results were observed in Morocco (Thévenot, 2006). In these studies, no details were provided on the macroscopic and microscopic preservation of bones and teeth. *Bubo* predation induces "little modification and a light degree of digestion" (Andrews, 1990) but *B. ascaphalus* was not studied. *Meriones* is less fragmented than other rodents in *B. ascalaphus* pellets from Algeria (Denys et al., 1996). Digestion by this predator induces very low surface modifications (Table 1), weak modifications of the microstructures and some changes in chemical composition. Further studies will be necessary to define the predation category of this nocturnal raptor but it may belong to a low modification one.

In Europe, *T. alba* belongs to the lowest category of modification (Andrews, 1990), and 8–13% of the incisors display signs of digestion. Bruderer and Denys (1999), have shown in a mauritanian assemblage that the percentage of digested incisors of Gerbilinae was higher than that of Murinae when compared to European assemblages. These data highlight the necessity to enlarge data for North Africa due to the different prey morphology and size. In Northwestern Africa, *T. alba* and owls from categories 1 and 2 have been studied for their diet, but not for the alterations they induce (e.g. Brosset, 1956; Saint Girons, 1973; Aulagnier et al., 1999; Baziz et al., 2001; Rihane, 2003, 2005; Sekour et al., 2010a).

The complexity of digestive effects has been shown by Leprince et al. (1979): for a given bird of prey, the gastric juices pH depends on the age of the bird, the number of meals during the day, etc. It seems also that the prey morphology and size may be factors of variability of the digestion on bone (Denys et al., 1996). Unfortunately, few studies are dedicated to such problems and data are very scarce.

In mature enamel, the low organic matrix content (4%) contains about 40% lipids and 60% proteins (collagen included) (Girija and Stephen, 2003; Açil et al., 2005). Experimental bleachings have shown that liquids are able to penetrate the outer enamel even when it is free of cracks or caries (Miranda et al., 2005). The mineral (apatite) component of the enamel is dissolved at a low pH. On the other hand, dentine is rich in organic content (up to 25%) in which collagen is one of the main components, and has a porous structure. Acidic gastric juices are able to cleave the organic matrices and to percolate in the tubules. Thus, both enamel and dentine are sensitive to the acidic pH of the gastric juices of birds of prey. From our data, it can be seen that the dentine is more altered than enamel, and that its range of variation in alteration is wider than that of enamel in the same teeth.

These results differ from the surface observations. In our pellet samples, some surface modifications of low intensity have been observed (Table 1), and the digestion first occurs on enamel on the tip of the tooth (pitting and dissolution) (Andrews, 1990; Stoetzel et al., 2011). These results attest that surface modifications, microstructural and chemical alterations are not necessarily related (Dauphin and Williams, 2007).

4.3. Early diagenesis

Most studies dealing with rodent teeth used laboratory raised animals, and data on wild animals are still rare. Such raised animals are overfed to increase the growth rate, and are allowed few physical exercises. Their teeth are often less mineralised than those of wild animals, especially for the ever-growing incisors or hypsodont teeth (unpublished data).

The two layered enamel and the uniserial pattern are common to *Rattus* and *Meriones*. In fresh samples, the crystallites within the enamel rod or prism are well visible on polished surfaces. The outer surfaces of the teeth extracted from pellets are not strongly etched, and sections do not reveal that they have been digested. Enamel and dentine structures seem to be intact. Not only it is not possible to infer the predator from the sections, but to distinguish between fresh and digested teeth is not an option at a microscale. Nevertheless, our data confirm that *T. alba* and *B. ascalaphus* belong to low modification categories of Andrews (1990), and that the unknown predators also belong to low categories of modifications.

Infrared maps show that *Rattus* and *Meriones* incisors share the same bulk composition. In all fresh teeth, EDJ is clearly visible and the main difference between enamel and dentine is shown by the 1100 cm^{-1} band (PO_4) and amide III. Despite the good preservation of the microstructure, the chemical composition of the teeth from pellets has been altered by the digestion. Moreover, the incisors extracted from pellets are heterogeneous in their state of preservation.

The comparison of chemical compositions shows that enamel and dentine of *Rattus* differ from those of the fresh *Meriones* (Table 2, S2). Because the composition of teeth depends on the species, but also from the diet, the origin of the difference cannot be assigned to a peculiar cause. Fe plays a role in the pigmentation of the enamel, as well as structural anomalies (Prime et al., 1984) and the "yellow orange" enamel of *Rattus* is rich in Fe. The orange incisors of *Meriones* are also rich in Fe. Dentine is more modified in pellets than the enamel. Moreover, the modifications in enamel and dentine differ: dentine has lost Mg and S, enamel has lost Ca and P. The comparison of the results of the star symbol analyses suggests that one of the teeth extracted from an unknown predator can be assigned to an owl (*T. alba*?).

4.4. Broader implications

Fossil bones and teeth are used to reconstruct palaeoenvironment, palaeodiet, phylogeny and geochronology through biogeochemical and isotopic analyses. However, the diagenetic factor is not always taken into account, especially the early diagenesis. Reconstructions of palaeodiet have been attempted by measuring elements influenced by the diet of the organism. The depletion of the organic components in dentine and enamel cannot be neglected: ^{14}C datation for example, can be biased. Not only is the mineral–organic ratio altered, but the composition of the organic matrix is also modified. How the DNA is affected is still unknown. The large DNA molecules seem to be degraded in small fragments: 200–450 bp for *T. alba* (Buś et al., 2014) or less in Moroccan samples (Geigl, pers. comm.). The concept of well-preserved samples is also an issue, since there is no direct relationship between the external aspect, the inner structure and the composition (Dauphin and Williams, 2007). A similar result was obtained by comparing the mineralisation category and chemical composition of fossil bones (Thomas et al., 2012). The detection of a predation signal in rodent fossil teeth, the main part of small mammal assemblages, may improve our knowledge of the sources of accumulation as well as some palaeoecological biases. However, it is not yet possible to characterize specific alterations related to each predator types due to the low number of available studies.

5. Conclusion

The inner microstructures of enamel and dentine of fresh or extracted from regurgitation pellets of different birds of preys of low modification categories do not seem modified by the digestive process. On the opposite, the composition of both tissues is altered in teeth extracted from pellets. Parameters such as crystallinity, organic/mineral ratios are modified, and the modifications are not identical in enamel and dentine. Despite only one tooth was examined for a given predator, from FTIR data, the affected parameters seem different according to the bird of prey. A second line of evidence comes from the elemental chemical composition of enamel and dentine. From this point of view, both tissues are altered by the digestion. The above results confirm that this early diagenesis depends upon the tissue (dentine alteration is stronger than that of enamel), and the predator. Similar results have been previously obtained using chemical composition. FTIR analysis adds data about crystallinity and organic components, so that the techniques are not redundant. Moreover, they can be done on the same samples. These results also demonstrate that the estimation of the changes in biogenic mineralised tissues cannot be reduced to a simplistic mineralogical equation.

Unfortunately, our knowledge of the variability of digestive processes of birds of prey is still rather limited, and to infer the state of preservation of modern digested teeth from a single criterion is not possible. Additionally, a relationship between the surficial alterations described by Andrews (1990) and the compositional changes has yet to be established. Our data show that a direct relationship between the microstructural and chemical changes is not predictable. Moreover, enamel is not immune to diagenetic alterations even in the predation stage. The potential impact of this specific post-mortem pre-depositional phase on subsequent fossilization processes needs further investigations, but these data suggest that predation was a contributory factor to the overall diagenetic process. As noted in Weiner (2010), "It is sometimes even tacitly assumed that enamel does not undergo diagenesis. This is not correct".

Uncited Reference

Dauphin et al. (1989), Denys et al. (1992), Denys and Patou-Mathis (2014), and Stoetzel (2013).

Acknowledgements

This work was realised thanks to post-doctoral grants (B. Farre, E. Stoetzel), the financial support of the Project ANR-09-PEXT-004 MOHMIE, and from the EC792 and ES42 ESRF grants. We thank Pr. Touria Benazzou (University Mohamed V- Agdal), Pr. A. Aouraghe (University of Oujda), Pr. M. Fekhaoui ("Institut Scientifique" of Rabat) and Pr. M. El Hassani, director of the "Institut Scientifique" (Rabat, Morocco) for logistic and field assistance. We are very grateful to Pr. Dr. A. Veis (Northwestern University, Feinberg School of Medicine, USA) who help us to improve the manuscript.

Appendix A. Supplementary data

Supplementary data associated with this article can be found, in the online version, at http://dx.doi.org/10.1016/j.micron.2015.04.010

References

Açil, Y., Mobasseri, A.E., Warnke, P.H., Terheyden, H., Wiltfang, J., Springer, I., 2005. Detection of mature collagen in human dental enamel. Calcif. Tissue Int. 76, 121–126.

Andrews, P., 1990. Owls, Caves and Fossils. Natural History Museum Publications, London.

Aulagnier, S., Thévenot, M., Gourves, J., 1999. Régime alimentaire de la chouette Effraie, *Tyto alba*, dans les plaines et reliefs du Maroc nord-Atlantique. Alauda 67, 271–351.

Baziz, B., Doumandji, S., Denys, C., Khemici, M., Benbouzid, N., Hamani, A., 2001. Données sur la chouette effraie *T. alba* Scopoli, 1796 (Aves, Tytonidae) en Algérie. Ornithologia algirica 1, 22–32.

Beddiaf, R., 2012. Etude du régime alimentaire de deux rapaces: le Hibou ascalaphe *Bubo ascalaphus* (Savigny, 1809) et la Chouette Chevêche Athene noctua (Scopoli, 1769) dans la région de Djanet (Tassili n'Ajjer, Algérie). Mém. Magister, Univ. Kasdi Merbah, Ouargala, Algérie, pp. 103.

Beniash, E., Metzler, R.A., Lam, R.S.K., Gilbert, P.U.P.A., 2009. Transient amorphous calcium phosphate in forming enamel. J. Struct. Biol. 166, 133–143.

Biche, M., Sellami, M., Libois, R., Yahiaoui, N., 2001. Régime alimentaire du Grand-duc du désert, *Bubo ascalaphus* dans la réserve naturelle de Mergueb (M'Sila, Algérie). Alauda 69, 554–557.

Boskey, A.L., 2007. Mineralization of bones and teeth. Elements 3, 387–393.

Boskey, A.L., Mendelsohn, R., 2005. Infrared spectroscopic characterization of mineralized tissues. Vib. Spectro. 38, 107–114.

Boskey, A.L., Pleshko Camacho, N., 2007. FT-IR imaging of native and tissue-engineered bone and cartilage. Biomaterials 28, 2465–2478.

Boukhamza, M., Hamdine, W., Thévenot, M., 1994. Données sur le régime alimentaire du Grand-duc ascalaphe (Bubo *bubo ascalaphus* en milieu steppique (Aïn Ouessera, Algérie). Alauda 62, 150–152.

Boyde, A., 1969. Correlation of ameloblast size with enamel prisms pattern: use of scanning electron microscope to make surface area measurements. Zeitschrift für Zellforschung und mikroskopische Anatomie 93, 583–593.

Boyde, A., 1978. Development of the structure of the enamel of the incisor teeth in the three classical subordinal groups of the Rodentia. In: Butler, P.M., Josey, K.A. (Eds.), Development, Function and Evolution of Teeth. Academic Press, London, pp. 43–58.

Brosset, M., 1956. Le régime alimentaire de l'Effraye *Tyto alba* au Maroc oriental. Alauda 24, 303–305.

Bruderer, C., Denys, C., 1999. Inventaire taxonomique et taphonomique d'un assemblage de pelotes d'un site de nidification de *T. alba* de Mauritanie. Bonner Zoologische Beiträge 48, 245–257.

Buś, M.M., Żmihorski, M., Romanowski, J., Balčiauskienė, L., Cichocki, J., Balčiauskas, L., 2014. High efficiency protocol of DNA extraction from Micromys minutus mandibles from owl pellets: a tool for molecular research of cryptic mammal species. Acta Theriologica 59, 99–109.

Dauphin, Y., Denys, C., 1988. Les mécanismes de formation des gisements de microvertébrés, 1- composition chimique élémentaire des tissus mineralisés de quelques rongeurs sauvages actuels. Revue de paléobiologie 7, 307–316.

Dauphin, Y., Denys, C., Denis, A., 1989. Les mécanismes de formation des gisements de microvertébrés. 2- Composition chimique élémentaire des os et dents de rongeurs provenant de pelotes de régurgitation. Bulletin du Museum national d'histoire naturelle, Paris, sect. A, zoologie, 4è sér. 11, 253–269.

Dauphin, Y., Denys, C., 1992. Diagenèse differentielle chez les rongeurs fossiles – validité des paramètres géochimiques pour les reconstitutions des régimes alimentaires. Palaeogeogr. Palaeoclimatol. Palaeoecol. 99, 213–223.
Dauphin, Y., Nespoulet, R., Stoetzel, E., El Haijraoui, M.A., Denys, C., 2012. Can colour be used as a proxy for paleoenvironmental reconstuctions based on archaeological bones? El Harhoura 2 (Morocco) case study. J. Taphonomy 10, 69–84.
Dauphin, Y., Williams, C.T., 2007. The chemical compositions of dentine and enamel from recent reptile and mammal teeth - variability in the diagenetic changes of fossil teeth. CrystEngComm. 9, 1252–1261.
Denys, C., 2011. Des référentiels en taphonomie des petits vertébrés: bilan et perspectives. In: Laroulandie, V., Mallye, J.B., Denys, C. (Eds.), Taphonomie des petits vertébrés: référentiels et transferts aux fossiles, Actes de la table ronde du RTP taphonomie, Talence 20-21 octobre 2009. BAR International Series, 2269, pp. 7–22.
Denys, C., Dauphin, Y., Rzebik-Kowalska, B., Kowalski, K., 1996. Taphonomic study of Algerian owl pellet assemblages and differential preservation of some rodents: palaeontological implications. Acta Zool. Cracoviensis 39, 103–116.
Denys, C., Kowalski, K., Dauphin, Y., 1992. Mechanical and chemical alterations of skeletal tissues in a recent Saharian accumulation of faeces from *Vulpes rueppelli* (Carnivora, Mammalia). Acta Zool. Cracoviensis 35, 265–283.
Denys, C., Patou-Mathis, M., 2014. Histoire de la taphonomie et concepts associés. In: Denys, C., Patou-Mathis, M. (Eds.), Manuel de taphonomie. Errance, Arles, France, pp. 13–26.
Elliott, J.C., Holcomb, D.W., Young, R.A., 1985. Infrared determination of the degree of substitution of hydroxyl by carbonate ions in human dental enamel. Calcif. Tissue Int. 37, 372–375.
Farre, B., Massard, P., Nouet, J., Dauphin, Y., 2014. Preservation of rodent bones from El Harhoura 2 cave (Morocco, Neolithic – Middle Palaeolithic): microstructure, mineralogy, crystallinity and composition. J. Afr. Earth Sci. 92, 1–13.
Fernandez-Jalvo, Y., Andrews, P., 1992. Small mammal taphonomy of Gran Dolina, Atapuerca (Burgos), Spain. J. Archaeol. Sci. 19, 407–428.
Fernandez-Jalvo, Y., Andrews, P., Sevilla, P., Requejo, V., 2014. Digestion versus abrasion features in rodent bones. Lethaia 47, 323–336.
Fernandez-Jalvo, Y., Denys, C., Andrews, P., Williams, C.T., Dauphin, Y., Humphrey, L., 1998. Taphonomy and palaeoecology of Olduvai Bed I (Pleistocene, Tanzania). J. Hum. Evol. 34, 137–172.
Geraads, D., 1998. Biogeography of circum-Mediterranean Miocene-Pliocene rodents: a revision using factor analysis and parsimony analysis of endemicity. Palaeogeogr. Palaeoclimatol. Palaeoecol. 137, 273–288.
Girija, V., Stephen, H.C., 2003. Characterization of lipid in mature enamel using confocal laser scanning microscopy. J. Dent. 31, 303–311.
Greene, E.F., Tauch, S., Webb, E., Amarasiriwardena, D., 2004. Application of diffuse reflectance infrared Fourier transform spectroscopy (DRIFTS) for the identification of potential diagenesis and crystallinity changes in teeth. Microchem. J. 76, 141–149.
Hollund, H.I., Ariese, F., Fernandes, R., Jans, M.M.E., Kars, H., 2013. Testing an alternative high-throughput tool for investigating bone diagenesis: FTIR in attenuated total reflection (ATR) mode. Archaeometry 55, 507–532.
Huang, C.M., Zhang, Q., Bai, S., Wang, C.S., 2007. FTIR and XRD analysis of hydroxyapatite from fossil human and animal teeth in Jinsha relict, Chengdu. Spectrosc. Spectral Anal. 27, 2448–2452.
Jacobs, Z., Roberts, R.G., Nespoulet, R., El Hajraoui, M.A., Debénath, A., 2012. Single-grain OSL chronologies for Middle Palaeolithic deposits at El Mnasra and El Harhoura 2, Morocco: implications for Late Pleistocene human-environment interactions along the Atlantic coast of northwest Africa. J. Hum. Evol. 62, 377–394.
Jaeger, J.J., 1977. Les rongeurs du Miocène moyen et supérieur du Maghreb. Palaeovertebrata 8, 1–166.
Janati Idrissi, N., Falguères, C., Haddad, M., Nespoulet, R., El Hajraoui, M.A., Debénath, A., Bejjit, L., Bahain, J.J., Michel, P., Garcia, T., Boudad, L., El Hammouti, K., Oujaa, A., 2012. Datation par ESR-U/Th combinées de dents fossiles de la région de Rabat-Témara: Grottes d'El Mnasra et d'El Harhoura 2. Quaternaire 23, 25–35.
von Koenigswald, W., 1985. Evolutionary trends in the enamel of rodent incisors. In: Luckett, P.W., Hartenberger, J.L. (Eds.), Evolutionary Relationships among Rodents. A Multidisciplinary Analysis, NATO Science Ser. A Life sciences, 92, pp. 403–422.
Korvenkontio, V.A., 1934. Mikroskopische Untersuchungen an Nagerincisiven unter Hinweis auf die Schmelzstruktur der Backenzähne. Ann. Zool. Soc. Zool. – Bot. Fennicae Vanamo 2, 1–274.
Leprince, P., Dandrifosse, G., Schoffeniels, E., 1979. The digestive enzymes and acidity of the pellets regurgitated by raptors. Biochem. System. Ecol. 7, 223–227.
Lesne, L., Thévenot, M., 1981. Contribution à l'étude du régime alimentaire du Hibou grand-duc Bubo *Bubo ascalaphus* au Maroc. Bulletin de l'Institut Scientifique de Rabat 5, 167–177.
Lopez-García, J.M., Agustí, J., Aouraghe, H., 2013. The small mammals from the Holocene site of Guenfouda (Jerada, Eastern Morocco): chronological and paleoecological implications. Hist. Biol. 25, 51–57.
Martin, T., 1997. Incisor enamel microstructure and systematics in rodents. In: von Koenigswald, W, Sander, PM (Eds.), Tooth Enamel Mirostructure. Balkema, Rotterdam, pp. 163–175.
Miranda, C.B., Pagani, C., Benetti, A.R., Matuda, F.S., 2005. Evaluation of the bleached human enamel by scanning electron microscopy. J. Appl. Oral Sci. 13, 204–211.
Nespoulet, R., El Hajraoui, M.A., Amani, F., Ben Ncer, A., Debenath, A., El Idrissi, A., Lacombe, J.P., Michel, P., Oujaa, A., Stoetzel, E., 2008. Palaeolithic and Neolithic occupations in the Temara Region (Rabat, Morocco): recent data on hominin contexts and behavior. Afr. Archaeol. Rev. 25, 21–39.
Pasteris, J.D., Wopenka, B., Valsami-Jones, E., 2008. Bone and tooth mineralization: why apatite? Elements 4, 97–104.
Paschalis, E.P., DiCarlo, E., Betts, F., Sherman, P., Mendelsohn, R., Boskey, A.L., 1996. FTIR microspectroscopic analysis of human osteonal bone. Calcif. Tissue Int. 59, 480–487.
Prime, S.S., MacDonald, D.G., Noble, H.W., Rennie, J.S., 1984. Effect of prolonged iron deficieny on enamel pigmentation and tooth structure in rat incisors. Arch. Oral Biol. 29, 905–909.
Reed, D.N., Barr, W.A., 2010. A preliminary account of the rodents from Pleistocene levels at Grotte des Contrebandiers (Smuggler's Cave), Morocco. Hist. Biol. 22, 286–294.
Rihane, A., 2003. Contribution à l'étude du régime alimentaire de la chouette effraie *Tyto alba* (Strigiformes, Tytonidae) dans les plaines semi-arides du Maroc atlantique. Alauda 71, 363–369.
Rihane, A., 2005. Contribution à l'étude du régime alimentaire de la chouette effraie *Tyto alba* dans les plaines semi-arides du Maroc (compléments). Go-South Bull. 2, 37–43.
Sahni, A., 1985. Enamel structure of early mammals and its role in evaluating relationships among rodents. In: Luckett, P.W., Hartenberger, J.L. (Eds.), Evolutionary Relationships Among Rodents. A Multidisciplinary Analysis, NATO Science Ser. A Life Sciences, 92, pp. 133–150.
Saint Girons, M.C., 1973. Le régime de l'effraie, *Tyto alba*, sur la côte atlantique du Maroc. Bulletin de la Société des Sciences Naturelles et Physiques du Maroc 53, 193–198.
Sekour, M., Baziz, B., Denys, C., Doumandji, S., Souttou, K., Guezoul, O., 2010a. Régime alimentaire de la Chouette chevêche (Athene noctua), de la Chouette effraie (*Tyto alba*), du Hibou moyen-duc (Asio otus) et du Hibou grand-duc ascalaphe (*Bubo ascalaphus*) dans la réserve naturelle de Mergueb (M'Sila, Algérie). Alauda 78, 103–117.
Sekour, M., Souttou, K., Denys, C., Doumandji, S., Abasa, L., Guezoul, O., 2010b. Place des ravageurs des cultures dans le régime alimentaire des rapaces nocturnes dans une région steppique à Ain el Hadjel. Leban. Sci. J. 11, 3–12.
Stoetzel, E., 2013. Late Cenozoic micromammal biochronology of northwestern Africa. Palaeogeogr. Palaeoclimatol. Palaeoecol. 392, 359–381.
Stoetzel, E., Campmas, E., Michel, P., Bougariane, B., Ouchaou, B., Amani, F., El Hajraoui, M.A., Nespoulet, R., 2014. Context of modern human occupations in North Africa: contribution of the Témara caves data. Quat. Int. 320, 143–161.
Stoetzel, E., Denys, C., 2009. Les microvertébrés d'Afrique du Nord: synthèse des travaux en néo- et paléotaphonomie. In: Laroulandie, V., Mallye, J.B., Denys, C. (Eds.), Taphonomie des Petits Vertébrés: Référentiels et Transferts aux Fossiles Actes de la Table Ronde du RTP Taphonomie, Talence 20-21 octobre. British Archaeological Reports, S2269, pp. 23–32.
Stoetzel, E., Marion, L., Nespoulet, R., El Hajraoui, M.A., Denys, C., 2011. Taphonomy and palaeoecology of the Late Pleistocene to Middle Holocene small mammal succession of El Harhoura 2 cave (Rabat-Temara, Morocco). J. Hum. Evol. 60, 1–33.
Thévenot, M., 2006. Aperçu du régime alimentaire du Grand-duc d'Afrique du Nord *Bubo ascalaphus* à Tata, Moyen Draa. Go-South Bull. 3, 28–30.
Vein, D., Thévenot, M., 1978. Étude sur le Hibou grand-duc Bubo *bubo ascalaphus* dans le moyen-Atlas marocain. Nos Oiseaux 34, 347–351.
von Koenigswald, W., Sanders, P.M., 1997. Glossary of terms used for enamel microstructures. In: Koenigswald, W.von, Sanders, P.M. (Eds.), Tooth Enamel Microstructure. Proc. Enamel Microstructure Workshop. Univ. Bonn, BALKEMA, Rotterdam, pp. 267–280.
Wahlert, J.H., 1968. Variability of rodent incisor enamel as viewed in thin section, and the microstructure of the enamel in fossil and recent rodent groups. Breviora 309, 1–18.
Wang, L., Fan, H., Liu, J., Dan, H., Ye, Q., Deng, M., 2007. Infrared spectroscopic study of modern and ancient ivory from sites at Jinsha and Sanxingdui, China. Mineral. Mag. 71, 509–518.
Warshawsky, H., 1971. A light and electron microscopic study of the nearly mature enamel of rat incisors. Anat. Rec. 169, 559–583.
Weber, D., 1965. Phase microscopic observations of rat incisor enamel. Am. J. Anat. 117, 233–249.
Weiner, S., 2010. Microarchaeology – Beyond the Visible Archaeological Record. Cambridge University Press, Cambridge.